



LAWRENCE
LIVERMORE
NATIONAL
LABORATORY

Plutonium desorption from mineral surfaces at environmental concentrations of hydrogen peroxide

J. D. Begg, M. Zavarin, A. B. Kersting

February 25, 2014

Environmental Science and Technology

Disclaimer

This document was prepared as an account of work sponsored by an agency of the United States government. Neither the United States government nor Lawrence Livermore National Security, LLC, nor any of their employees makes any warranty, expressed or implied, or assumes any legal liability or responsibility for the accuracy, completeness, or usefulness of any information, apparatus, product, or process disclosed, or represents that its use would not infringe privately owned rights. Reference herein to any specific commercial product, process, or service by trade name, trademark, manufacturer, or otherwise does not necessarily constitute or imply its endorsement, recommendation, or favoring by the United States government or Lawrence Livermore National Security, LLC. The views and opinions of authors expressed herein do not necessarily state or reflect those of the United States government or Lawrence Livermore National Security, LLC, and shall not be used for advertising or product endorsement purposes.

1 **Disclaimer**

2 This document was prepared as an account of work sponsored by an agency of the United States
3 government. Neither the United States government nor Lawrence Livermore National Security, LLC, nor
4 any of their employees makes any warranty, expressed or implied, or assumes any legal liability or
5 responsibility for the accuracy, completeness, or usefulness of any information, apparatus, product, or
6 process disclosed, or represents that its use would not infringe privately owned rights. Reference herein to
7 any specific commercial product, process, or service by trade name, trademark, manufacturer, or
8 otherwise does not necessarily constitute or imply its endorsement, recommendation, or favoring by the
9 United States government or Lawrence Livermore National Security, LLC. The views and opinions of
10 authors expressed herein do not necessarily state or reflect those of the United States government or
11 Lawrence Livermore National Security, LLC, and shall not be used for advertising or product
12 endorsement purposes.

13 LLNL-JRNL-650559

14

15

16

17

18

19

20 Plutonium desorption from mineral surfaces at
21 environmental concentrations of hydrogen peroxide

22 *James D. Begg*, Mavrik Zavarin, Annie B. Kersting*

23 Glenn T. Seaborg Institute, Physical & Life Sciences, L-231, Lawrence Livermore National
24 Laboratory,
25 Livermore, CA 94550

26 *Corresponding Author: Begg2@llnl.gov

27

28

29

30

31

32

33

34

35

36

37

38

39

40 **ABSTRACT**

41 Knowledge of Pu adsorption and desorption behavior on mineral surfaces is crucial for
42 understanding its environmental mobility. Here we demonstrate that environmental
43 concentrations of H₂O₂ can affect the stability of Pu adsorbed to goethite, montmorillonite and
44 quartz across a wide range of pH values. In batch experiments where Pu(IV) was adsorbed to
45 goethite for 21 days at pH 4, 6, and 8, the addition of 5 – 500 μM H₂O₂ resulted in significant Pu
46 desorption. At pH 6 and 8 this desorption was transient with re-adsorption of the Pu to goethite
47 after 30 days. At pH 4, no Pu re-adsorption was observed. Experiments with both quartz and
48 montmorillonite at 5 μM H₂O₂ desorbed far less Pu than in the goethite experiments highlighting
49 the contribution of Fe redox couples in controlling Pu desorption at low H₂O₂ concentrations.
50 Plutonium(IV) adsorbed to quartz, and subsequently spiked with 500 μM H₂O₂ resulted in
51 significant desorption of Pu, demonstrating the complexity of the desorption process. Our results
52 provide the first evidence of H₂O₂ catalyzed desorption of Pu(IV) from mineral surfaces. We
53 suggest that this reaction pathway coupled with environmental levels of hydrogen peroxide may
54 contribute to Pu mobility in the environment.

55 **KEYWORDS**

56 Plutonium, desorption, hydrogen peroxide

57

58

59

60

61 INTRODUCTION

62 The production and testing of nuclear weapons, nuclear accidents and authorized discharges of
63 radionuclides have all contributed to a global legacy of plutonium (Pu) contamination in the
64 environment.¹⁻⁴ Pu contamination in the environment is a topic of key concern because of its
65 radiological toxicity and long half-life (24,100 years for ²³⁹Pu). A wide array of factors can
66 significantly influence Pu mobility in natural systems including redox processes ^{5, 6}; colloid-
67 facilitated transport processes ⁷⁻⁹; solubility effects ^{10, 11}; sorption/desorption rates and affinities
68 for natural mineral surfaces ¹²⁻¹⁴; and interactions with natural organic matter (including bacteria)
69 ^{15, 16}. One of the outstanding issues currently limiting the development of reliable predictive
70 transport models involves understanding the rates and mechanisms of Pu sorption to, and
71 desorption from, mineral surfaces in the presence of water.

72 Under environmental conditions Pu can exist in multiple oxidation states (Pu(VI), Pu(V), Pu(IV),
73 and Pu(III)) with each oxidation state displaying a unique solubility¹⁰ and sorption affinity.^{12, 17-19}
74 Importantly, redox kinetics can be rate limited which may lead to transient, non-equilibrium
75 conditions.^{12, 14} Pu(VI) may occur in highly oxidic waters, such as rainwaters, but it is expected to
76 rapidly reduce to Pu(V) in most other natural waters.^{20, 21} In oxidic environments, such as in
77 surface waters, Pu in the aqueous phase is predominantly expected to occur in the pentavalent
78 state.^{5, 20, 21} Due to effective charge considerations, Pu(V) is also expected to be the most mobile
79 oxidation state of Pu, displaying a low adsorption affinity for mineral surfaces. In the presence of
80 organic and inorganic material (including mineral surfaces), Pu(V) has been shown to reduce to
81 Pu(IV).^{18, 22-25} For example, the adsorption of Pu(V) to the iron oxyhydroxide mineral goethite
82 (α -FeOOH) is thought to result in the reduction of Pu(V) to Pu(IV) on the mineral surface driving
83 further adsorption of aqueous Pu(V).^{18, 23} Similar surface-mediated redox processes have been

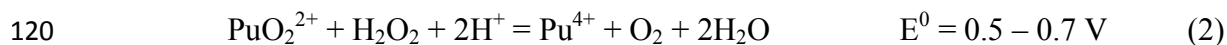
84 observed on montmorillonite and quartz surfaces.^{12, 26, 27} In suboxic subsurface waters, Pu is
85 predominantly expected to occur in the tetravalent state which has been shown to have a far
86 greater adsorption affinity for mineral surfaces than either Pu(III), Pu(V) or Pu(VI).^{5, 18, 21, 25, 28, 29}
87 Therefore, the Pu(IV) oxidation state is likely to be the most important oxidation state of Pu
88 associated with mineral surfaces. Pu(III) has only been detected under simulated anoxic
89 environmental conditions.^{28, 30, 31}

90 The desorption of Pu from mineral surfaces has received less attention than adsorption although
91 it will also ultimately play a key role in determining the extent of aqueous Pu environmental
92 transport. Typically, batch desorption experiments demonstrate that Pu largely remains
93 associated with the mineral surface. For example, Pu batch desorption experiments with goethite
94 and hematite have indicated that less than 1% of the Pu associated with the mineral surface will
95 be desorbed.³² Similarly, experiments with sediments from the Esk Estuary, UK showed that
96 about 5% of Pu associated with the sediments (which was predominantly in the Pu(III)/(IV)
97 oxidation state on the sediment surface) could be desorbed in batch experiments.³³ Similar
98 values were measured from Pu desorbed from Aiken, SC sediments³⁴ where approximately 1-9%
99 of adsorbed Pu was removed in batch experiments across a pH range from 2.4-8.4. Greater
100 extents of Pu desorption have been reported for montmorillonite and silica, where up to 20% of
101 Pu was desorbed after ~300 days in batch experiments at pH ~8.¹⁴

102 The oxidation state of Pu is also important in controlling both the rate and extent of Pu
103 desorption from mineral surfaces.^{14, 32-34} For example, the Pu, which was initially present on the
104 solid surface as Pu(IV), in the Aiken, SC sediments was found to be present in solution as Pu(V)
105 following a desorption period of 33 days.³⁴ In this case it was proposed that the oxidation of
106 Pu(IV) to Pu(V) on the mineral surface was the mechanism behind the Pu(IV) desorption.

107 Further, the desorption of Pu(IV) from Irish Sea sediments was found to increase when they were
108 exposed to natural sunlight.³⁵ The sunlight was thought to cause the photooxidation of surface
109 Pu(IV) to Pu(V) which was subsequently more readily desorbed. This redox driven
110 remobilization is consistent with the behavior of other redox active radionuclides, such as Tc, Np
111 and U, where oxidation of reduced, solid-associated species results in their remobilization.³⁶⁻⁴⁰

112 High concentrations of H₂O₂ (~0.01 – 0.1 M) are known to alter the oxidation state of Pu^{6,41} and
113 are used in the purification and separation of waste streams as well as the preparation of Pu stock
114 solutions for use in experimental work (e.g. Clark et al. 2007).⁴² Hydrogen peroxide can be used
115 to reduce Pu(V) or Pu(VI) to Pu(IV) and to precipitate Pu(IV) from acidic solution.^{41, 43}
116 Oxidation of Pu(OH)₄ by H₂O₂ in 4 M NaOH solution has also been demonstrated.⁴⁴ These
117 results are consistent with half-cell reactions which demonstrate that both oxidation and
118 reduction of Pu by hydrogen peroxide is possible (Equations 1 and 2).⁴⁵

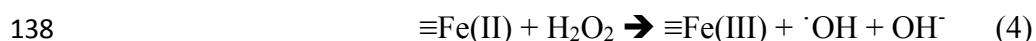
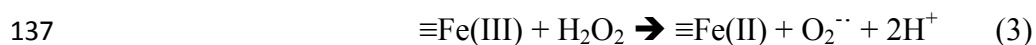


121 It has been suggested that in seawater and at concentrations as low as 1×10^{-5} M, H₂O₂ may
122 enhance the reduction of Pu(V) to Pu(IV) thus potentially decreasing the mobility of Pu(V)
123 species.⁶

124 Hydrogen peroxide is present in natural water bodies as a result of various processes including
125 photochemical reactions mediated by natural organic matter, input from rainwater, and metabolic
126 processes of fungi and bacteria.⁴⁶⁻⁴⁹ Concentrations up to 40 μM have been measured in
127 rainwater while in soils, H₂O₂ generated by fungi and bacteria can result in concentrations
128 between 2 and 15 μM in the surrounding microenvironment.^{46, 48-51} Indeed, it has recently been
129 proposed that H₂O₂ produced by subsurface bacteria may enhance the oxidation of contaminant

130 iodide species with associated implications for the environmental mobility of ^{129}I .⁵² Finally, in
131 nuclear waste repository scenarios, groundwater adjacent to spent nuclear fuel will be exposed to
132 ionizing radiation resulting in the production of H_2O_2 at concentrations of 1 – 1000 μM .⁵³⁻⁵⁵

133 It has been demonstrated that the decomposition of H_2O_2 is catalyzed in the presence of
134 Fe(II)/(III) species resulting in the production of reactive oxygen species (ROS) such as $\text{O}_2^{\cdot\cdot}$ and
135 OH^{\cdot} .⁵⁶⁻⁵⁹ The generation of these ROS is pH dependent and is an area of active research.
136 Illustrative reactions are shown in Equations 3 and 4.



139 The ROS can enhance oxidation of organic matter or metals and may be more effective oxidizers
140 than H_2O_2 alone.^{56-58, 60} This oxidation can also extend to species, such as As(III) , adsorbed to the
141 surface of iron(hydr)oxide minerals, and may exert an important control on their environmental
142 mobility.^{58, 59} Further, recent work has demonstrated that alpha radiolysis induced by ^{238}Pu can,
143 in the presence of Fe(II) , lead to the production of a sufficient concentration of H_2O_2 to cause the
144 oxidative dissolution of PuO_2 .⁵⁵ To our knowledge there have been no studies examining the
145 effect of H_2O_2 on Pu adsorbed to the surface of common minerals at environmentally relevant
146 H_2O_2 concentrations.

147 Here we demonstrate that the desorption of Pu(IV) adsorbed onto mineral surfaces is caused by
148 the presence of environmental concentrations of H_2O_2 . In our study, Pu(IV) was adsorbed to the
149 surface of goethite (αFeOOH); montmorillonite (2:1 dioctahedral clay), and high purity quartz
150 (SiO_2) for a minimum of 21 days. H_2O_2 was then spiked into Pu -mineral suspensions and
151 aqueous Pu concentration monitored. H_2O_2 concentrations in the experiments ranged from 5 –

152 500 μM and are broadly comparable to measured rainwater values ($< 2 \mu\text{M}$ to $> 40 \mu\text{M}$),
153 concentrations generated by some bacteria (2- 15 μM) and concentrations likely to exist in
154 nuclear repository environments as a result of radiolysis reactions (1 – 1000 μM).^{46, 48-51}

155 **MATERIALS AND METHODS**

156 *Plutonium stock preparation*

157 A ^{238}Pu stock (99.8% ^{238}Pu , 0.1% ^{241}Pu , and 0.1% ^{239}Pu by activity) was used in all experiments.
158 The Pu stock solution was purified using an anion exchange resin (BioRad AG 1 \times 8, 100–200
159 mesh) pre-conditioned with 8 M HNO_3 . Prior to loading on the resin, Pu was reacted with
160 NaNO_2 to reduce it to Pu(IV). The Pu was loaded on the resin in 8 M HNO_3 , washed with 3
161 column volumes of 8 M HNO_3 , and then eluted in 0.1 M HCl .⁶¹ The oxidation state of the Pu
162 stock was checked with a LaF_3 precipitation method⁶⁵ and found to be $> 99 \%$ Pu(III)/(IV).

163 *Mineral preparation*

164 All solutions were prepared using ultrapure water (Milli-Q Gradient System, $>18 \text{ M}\Omega\text{-cm}$) and
165 ACS grade chemicals without further purification. The SWy-1 montmorillonite (Source Clays
166 Repository of the Clay Minerals Society) was Na-homoionized and treated to remove organic
167 matter and free iron oxides. Details regarding this and the preparation of goethite were reported
168 previously.^{12, 26, 61, 62} The Iota 8 high purity quartz was obtained from Unimin Corporation
169 (Spruce Pine, NC) and was ground in a ball mill to increase surface area; no other pre-treatment
170 was performed. Surface areas were $20.6 \pm 0.6 \text{ m}^2 \text{ g}^{-1}$ for goethite, $31.5 \pm 0.2 \text{ m}^2 \text{ g}^{-1}$ for
171 montmorillonite and $2.1 \pm 0.2 \text{ m}^2 \text{ g}^{-1}$ for quartz ($\text{N}_2(\text{g})$ -BET, Quadrasorb SI). The amount of
172 extractable Fe in the montmorillonite removed by 0.5 N HCl was 530 ppm.^{12, 63} The Fe content

173 of Iota 8 high purity quartz is reported to be < 0.05 ppm (Unimin Corporation; Spruce Pine,
174 NC).⁶⁴

175 *Hydrogen peroxide desorption experiments*

176 Minerals were initially suspended in a 0.7 mM NaHCO₃, 5 mM NaCl buffer solution. Goethite
177 suspensions were prepared with a solid-solution concentration of 0.1 g L⁻¹, montmorillonite and
178 quartz suspensions had a concentration of 1 g L⁻¹. Dilute HCl and NaOH were used to adjust the
179 pH of the mineral suspensions to 4, 6, and 8. Suspensions were equilibrated for 48 hours under
180 atmospheric conditions and then spiked with Pu(IV) to a final concentration of 3 × 10⁻¹⁰ M which
181 is expected to be below the solubility of Pu(IV). The pH was readjusted accordingly and the
182 suspensions allowed to equilibrate in the dark at room temperature for 21 days.

183 Following this equilibration period, aliquots of the suspension were removed and centrifuged at
184 10,000 × g for 30 minutes to achieve a particle size cut-off of 60 nm. The Pu concentration in the
185 supernatant was determined by liquid scintillation counting (LSC; Packard Tri-Carb TR2900
186 LSA and Ultima Gold cocktail). A 35 mL aliquot of the original suspensions was transferred to a
187 clean Nalgene Oak Ridge polycarbonate centrifuge tube and spiked with a H₂O₂ stock prepared
188 by dilution of a 30 % H₂O₂ solution with Milli-Q water just before use. The concentration of the
189 H₂O₂ stock was verified by measuring its absorbance at 240 nm.⁶⁶ Final H₂O₂ concentrations
190 were 5, 50 and 5 μM in goethite experiments, 5 and 500 μM in quartz experiments and 5 μM in
191 montmorillonite experiments. The tubes were wrapped in aluminum foil to minimize
192 photochemical reactions and placed on an orbital shaker at 125 rpm at room temperature.

193 To measure desorption of Pu from mineral surfaces, aliquots of the suspensions were withdrawn,
194 centrifuged and the Pu concentration in the supernatant determined by LSC. Pu desorption was
195 typically monitored over a 30 day (720 hour) period. Supernatant Fe_{total} concentration in goethite

196 experiments at early timepoints was measured using the Ferrozine method described by Viollier
197 et al.⁶⁷

198 To characterize H₂O₂ decomposition in the presence of goethite, a set of Pu-free goethite
199 experiments was performed at pH 4, 6, and 8 with 50 μM H₂O₂. The H₂O₂ concentration in the
200 supernatant was measured as a function of time using Amplex Red reagent (Life Technologies,
201 CA).⁶⁸ Standard calibrations were run at each sampling point and returned R² values of 0.99 or
202 better (detection limit is 0.1 μM).⁶⁹

203 *Flow cell experiment*

204 To complement the batch experiments, a flow cell experiment was performed with goethite at pH
205 8. The flow cell set up was similar to that described previously for Np(V) reaction with
206 goethite.⁶² The flow cell was made of Teflon and had a volume of 20 mL. Prior to use, the cell
207 was washed with 10% HCl and MQ water. A 20 mL aliquot of the 21 day Pu-goethite
208 equilibrated suspension at pH 8 was placed in the flow cell and 0.7 mM NaHCO₃, 5 mM NaCl
209 buffer solution at pH 8 was pumped through the cell at a rate of 0.4 mL min⁻¹ (retention time of
210 50 minutes) for 3 chamber volumes. After this period, the influent solution was changed to a
211 buffer solution spiked with 10 μM H₂O₂ at a rate of 0.4 mL min⁻¹ for 7 chamber volumes.
212 Effluent fractions were collected on a Spectra/Chrom CF-1 fraction collector and the volumes
213 determined gravimetrically. Pu concentration was determined via LSC as described previously.

214 **RESULTS AND DISCUSSION**

215 Two terms are used to describe the sorption/desorption behavior of Pu in the current work. The
216 first of these is K_d (mL g⁻¹), which was calculated after the 21 day adsorption period from the
217 bulk Pu suspension concentration (C_{Bulk}, M), supernatant Pu concentration (C₀, M) and the

218 mineral suspension concentration ($[\text{mineral}]$, g mL^{-1}) as follows:

$$219 \quad K_d = \frac{C_{\text{Bulk}} - C_0}{C_0} \frac{1}{[\text{mineral}]} \quad (5)$$

220 Typically, K_d values are used to imply an equilibrium distribution coefficient. However in these
221 experiments equilibrium was most likely not achieved because of the complexity of Pu oxidation
222 state transformations on both mineral surfaces and in solution. As a result, we consider K_d in this
223 work to be a conditional K_d used simply to characterize the distribution of Pu between the solid
224 and the aqueous phase.

225 The second term is ‘desorbed Pu’ (C_{des} , M) which refers to the concentration of Pu desorbed
226 from the mineral surface and is calculated by subtracting the aqueous Pu concentration at the
227 time suspensions were spiked with H_2O_2 from the concentration of Pu at each time point. C_{des}
228 was calculated as:

$$229 \quad C_{\text{des}} = C_t - C_0 \quad (6)$$

230 Where C_t (M) is the concentration of Pu in solution at the sampling timepoint and C_0 (M) is
231 the concentration of Pu in the supernatant after the 21 day adsorption equilibration period. C_{des} is
232 used to allow comparison of the absolute concentration of Pu desorbed from the mineral surface
233 in these experiments because the initial amount of Pu adsorbed to the mineral surface varies as a
234 function of pH and mineral type. Because of the way C_{des} is calculated, it is possible to obtain
235 negative values for this term as re-adsorption processes can result in Pu solution concentrations
236 falling below values measured at the start of the H_2O_2 experiments.

237 *Adsorption of Pu(IV) to goethite, montmorillonite and quartz*

238 The adsorption of Pu(IV) to all minerals following the 21 day adsorption equilibration period is
239 reported in terms of $\log K_d$ in Table 1. These data show that the adsorption of Pu(IV) is strongly

240 affected by both pH and mineral type. Furthermore, the pH-dependence is unique to each
241 mineral. In the case of goethite, the extent of adsorption was lowest at pH 4 and highest at pH 8.
242 For montmorillonite, the highest Pu(IV) adsorption is at pH 4 after which adsorption decreases
243 with increasing pH. Pu(IV) sorption to quartz was lower than for montmorillonite and goethite
244 and shows a maximum K_d value at pH 6. The K_d values obtained in the current work for goethite
245 and quartz are broadly consistent with those calculated from previous adsorption studies for
246 goethite¹⁸ and quartz²⁷. For montmorillonite, which to our knowledge has been the subject of
247 fewer Pu adsorption studies, the log K_d value at pH 8 of 4.48 is similar to the value of 4.32
248 obtained previously in a comparable isotherm experiment with 10^{-10} M Pu(IV).¹²

249 *Pu(IV) – Goethite – H₂O₂ Interactions*

250 Addition of H₂O₂ to systems containing Pu(IV) adsorbed to goethite resulted in the desorption of
251 Pu(IV) from the goethite surface (Figure 1). The extent of desorption showed a pH dependency
252 such that the amount of Pu desorbed at pH 4 > pH 6 >> pH 8. At pH 4, the Pu continues to be
253 removed from the goethite surface throughout the experiment (720 hours). In contrast, at pH 6
254 and 8 desorption had stopped and re-adsorption of Pu from solution had started to occur by the
255 end of the experiment as evidenced by a decline in desorbed Pu concentration.

256 In batch experiments, the maximum desorption of Pu was observed at pH 4 with a H₂O₂
257 concentration of 500 μ M where 76% of the Pu initially associated with the goethite was
258 desorbed. The lowest maximum desorption observed was at pH 8 with a H₂O₂ concentration of 5
259 μ M in which 1.8 % of the surface Pu was desorbed after 288 hours. This value is significantly
260 larger than the < 1% desorption of Pu from goethite at pH 8.25 reported by Lu et al.³²
261 Importantly, for experiments at circumneutral pH values, significant desorption of Pu was
262 observed at environmentally relevant concentrations of 5 (pH 6, 32.5%; pH 8, 5.6%) and 50 μ M

263 (pH 6, 36.4%; pH 8, 1.8%) H₂O₂.⁴⁸⁻⁵⁰ Thus our results suggest that the desorption of Pu(IV)
264 adsorbed to goethite surfaces in natural environments could be catalyzed by the presence of
265 H₂O₂.

266 Apparent rates of Pu desorption from goethite in the first 4 hours of the experiment were
267 calculated and are plotted as a function of H₂O₂ concentration in Supporting Information (SI)
268 Figure S1. For experiments at pH 4 and 6, the early-time rates of Pu desorption are similar. In all
269 experiments, the rates are substantially greater at 50 and 500 μM H₂O₂ than at 5 μM. However, a
270 simple first order dependence on H₂O₂ concentration is not observed. This suggests that H₂O₂
271 may not be the rate-limiting species for desorption but that it may be a product of H₂O₂
272 decomposition which controls Pu desorption. At pH 8, apparent desorption rates are much lower
273 than at pH 4 and pH 6 for all H₂O₂ concentrations. The desorption rate at pH 8 with a H₂O₂
274 concentration of 5 μM is again lower than the rate at 50 μM and 500 μM but the difference is
275 much less marked than for experiments at pH 4 and 6.

276 To examine the relationship between H₂O₂ decomposition and Pu desorption, H₂O₂
277 concentrations were measured in Pu-free goethite experiments spiked with 50 μM H₂O₂. Figure
278 2 shows that a decline in H₂O₂ concentration occurs over time at all pH values. After 192 hours,
279 over 94% of H₂O₂ had been lost from solution at all pH values. Pseudo-first order rate constants
280 were calculated for the first 96 hours of H₂O₂ loss from solution. Data were surface area
281 normalized in order to facilitate comparison with other work. Rates were 0.019 h⁻¹ m⁻², 0.013 h⁻¹
282 m⁻² and 0.002 h⁻¹ m⁻² at pH 4, 6 and 8, respectively. A pH dependency on the rate of H₂O₂
283 decomposition in the presence of an iron oxyhydroxide mineral has been observed previously.^{59,}
284 ^{70, 71} Our rates of H₂O₂ decomposition are comparable to previously published surface area

285 normalized H_2O_2 decomposition rates in the presence of goethite at pH ~ 7 of $0.0098 \text{ h}^{-1} \text{ m}^{-2}$ and
286 $0.0012 \text{ h}^{-1} \text{ m}^{-2}$.^{70, 71}

287 Comparison of these parallel Pu-free experiments (Figure 2) with Pu-containing experiments at
288 $50 \mu\text{M}$ H_2O_2 (Figure 1) indicates that the apparent rate/extent of Pu desorption is broadly
289 proportional to the rate of H_2O_2 loss. For example, H_2O_2 decomposition rates at pH 4 and pH 6
290 are comparable to each other and are significantly greater than the rate at pH 8. Similarly, initial
291 Pu desorption rates at pH 4 and 6 are alike and greater than the rate at pH 8. It is important to
292 note that whilst the parallel Pu-free experiment at pH 4 shows that H_2O_2 has been largely
293 removed from solution after 100 hours of reaction time (Figure 2), in the equivalent Pu-
294 containing experiment, Pu continues to be desorbed from the goethite surface (Figure 1). In
295 contrast, at pH 8, the Pu concentration in solution begins to fall after 48 hours despite the parallel
296 H_2O_2 experiment indicating that there will still be significant H_2O_2 remaining in solution at this
297 time (Figure 1; Figure 2). This suggests that it is H_2O_2 decomposition products and not H_2O_2 that
298 catalyze Pu desorption. Further work is needed to elucidate the species responsible for catalyzing
299 Pu desorption at different pH values.

300 *Mechanisms for Pu desorption*

301 To test whether goethite dissolution was responsible for Pu desorption from goethite, the
302 concentration of Fe in solution was measured at early time points. However, no significant Fe
303 was detected in solution during the first 48 hours of the experiment via spectrophotometric
304 analysis (estimated detection limit $0.3 \mu\text{M}$). Further, measurement of all the supernatants by ICP-
305 MS after 12 days of reaction showed that Fe concentrations were below $2 \mu\text{M}$ and did not differ
306 significantly from pre H_2O_2 spike concentrations (data not shown). This indicates that the
307 observed desorption of Pu is not the result of goethite dissolution.

308 It is likely that changes in Pu oxidation state will contribute to the desorption of Pu(IV) in these
309 experiments given that Pu(III), Pu(V) and Pu(VI) species all have a lower sorption affinity for
310 goethite than Pu(IV).^{18, 25, 29} Due to the low Pu concentrations used in this study, the complex
311 nature of aqueous Pu oxidation state distribution, and the relatively fast timescales of the Pu
312 desorption observed here, traditional indirect methods of assessing Pu oxidation state in solution
313 (e.g. LaF3 precipitation, solvent extraction) were unable to definitively characterize these
314 systems. However, the results of aqueous Pu oxidation state measurements in experiments at pH
315 4 and pH 6 at 500 μM H_2O_2 , where the most Pu desorption is observed, show that the
316 predominant aqueous oxidation state changes from Pu(III)/(IV) to Pu(V)/(VI) over the course of
317 the experiment. A more detailed discussion of these data is included in the SI. Previously,
318 Fenton-type reactions between H_2O_2 and Fe(III) have been shown to produce ROS capable of
319 altering the oxidation state of As(III) adsorbed to a ferrihydrite leading to potential changes in its
320 sorption behavior.⁵⁹ Thus, it is likely that H_2O_2 interaction with Fe(III) results in the production
321 of ROS which act to alter the oxidation state of sorbed Pu(IV), most likely to Pu(V) or Pu(VI),
322 leading to its desorption from the mineral surface.

323 *Re-adsorption of Pu by goethite*

324 As mentioned previously, a noticeable aspect of the pH 6 and pH 8 desorption plots in Figure 1
325 is that at all H_2O_2 concentrations investigated, a percentage of the Pu which was initially
326 desorbed is subsequently re-adsorbed on the goethite surface. The re-adsorption was not
327 observed at pH 4 over the timescale of these experiments (30 days). The initial desorption
328 followed by re-adsorption of Pu suggests that there are at least two competing processes with
329 different kinetic rates occurring in these systems: a ‘forward’ H_2O_2 -catalyzed Pu desorption
330 process and a ‘reverse’ Pu re-adsorption process. Thus the apparent extent of desorption at any

331 one time in these experiments is both a function of the ‘forward’ H₂O₂ driven desorption (H₂O₂-
332 catalyzed Pu(IV) oxidation and desorption) and also of the rate of the ‘reverse’ re-
333 adsorption/surface mediated reduction. The faster re-adsorption/surface mediated reduction
334 observed here with increasing pH is consistent with the pH-dependent surface mediated Pu(V)
335 reduction rates on goethite reported by Powell et al. (2005).²³

336 Pu adsorption to goethite exhibits a pH dependency in these experiments and is greatest at pH 8
337 (Table 1). Additionally, the reaction of H₂O₂ with Fe(III) and the nature of the ROS formed has
338 been shown to be pH dependent.⁵⁹ Thus we propose that the lower level of desorption observed
339 at pH 8 is a function of both the limited efficacy of the forward H₂O₂-catalyzed desorption and
340 the strong adsorption affinity of Pu for goethite at this pH. Further the re-adsorption, which is
341 also seen at pH 6, likely results from a loss of effective ROS species in the batch system and
342 hence a loss of driver for the forward desorption reaction. In contrast, at pH 4, the forward
343 reaction is not only more effective but the adsorption affinity of Pu (especially Pu(V)) for
344 goethite is much lower than at pH 8.²³ This interplay of forward and reverse processes is likely to
345 have implications for the H₂O₂ influenced mobility of Pu in natural environments.

346 *Goethite flow cell experiment*

347 The flow cell experiment was performed with 10 μM H₂O₂ to confirm that the re-adsorption of
348 Pu observed in the batch goethite experiments at pH 8 was caused by a decline in H₂O₂/ROS
349 concentration. Figure 3 shows the cumulative fraction of surface Pu desorbed from the goethite
350 during the flow cell experiment. Minimal Pu was desorbed from the goethite when the influent
351 solution was the 0.7 mM NaHCO₃, 5 mM NaCl buffer solution at pH 8 (Figure 3). However,
352 when the influent solution was spiked with H₂O₂ (indicated by the dashed red line in Figure 3) a
353 significantly higher concentration of Pu was desorbed. Continuous desorption of Pu from the

354 goethite was observed for the duration of the flow cell experiment. At the termination of the
355 experiment, the amount of surface Pu desorbed was 3.2% compared to batch experiments at pH 8
356 with 5 and 50 μM H_2O_2 where maximum surface desorption was 1.8 % and 5.6 %, respectively.
357 The continuous removal of Pu from the goethite surface as opposed to the re-adsorption in the
358 batch experiments also demonstrates that it is a decline in the efficiency of the ‘forward’ H_2O_2 -
359 catalyzed desorption which leads to the re-adsorption of Pu seen in batch experiments at pH 8.
360 From an environmental standpoint, this suggests that the continued presence of H_2O_2 in the
361 environment will lead to significant desorption of Pu from the surface of iron containing
362 minerals at circumneutral pH. In contrast, transient production of H_2O_2 by natural processes
363 would result in a temporary desorption of Pu.

364 *Pu(IV)-quartz- H_2O_2 and Pu(IV)-montmorillonite- H_2O_2 interactions*

365 Plutonium- H_2O_2 desorption experiments were also performed with quartz and montmorillonite at
366 a H_2O_2 concentration of 5 μM . These experiments were carried out to determine if environmental
367 concentrations of H_2O_2 could catalyze desorption of Pu from a mineral surface lacking an
368 obvious catalytic iron species. Figure 4 shows that H_2O_2 -catalyzed desorption of Pu from the
369 quartz and montmorillonite surfaces occurs to some degree and in a transient manner at all three
370 pH values. However, the extent of desorption is much less pronounced than that observed in the
371 corresponding goethite experiments. We note the increased scatter in the data in the quartz
372 experiments which we attribute in part to the lower initial adsorption of Pu(IV) onto quartz. The
373 desorption of Pu from both quartz and montmorillonite was transitory at all pH values with Pu
374 concentrations declining to values at least equal to or less than initial solution concentrations by
375 the end of the experiment leading to negative desorbed Pu concentrations in Figure 4.

376 Although these results suggest that the presence of H_2O_2 at environmental concentrations can
377 catalyze desorption of Pu from quartz and montmorillonite, it also highlights the importance of
378 reactive Fe in the desorption process at low H_2O_2 concentrations. Future work is planned to
379 investigate whether ROS formed by the decomposition of H_2O_2 in the presence of goethite can
380 enhance the desorption of Pu from adjacent mineral surfaces such as montmorillonite and quartz.

381 A final experiment was performed with quartz and H_2O_2 at 500 μM H_2O_2 . SI Figure S3 shows
382 that Pu desorption was much more pronounced at this higher H_2O_2 concentration. The extent of
383 Pu desorption is surprising given that there is no obvious source of catalyst for the Fenton-type
384 heterogeneous oxidation which is posited to drive Pu desorption from goethite. Measurement of
385 Si in solution after 12 days of reaction indicated that some dissolution of quartz occurred in these
386 experiments following addition of H_2O_2 (data not shown) so we cannot rule out a dissolution
387 driven desorption process in these experiments. Nonetheless, the data indicate that given
388 sufficient H_2O_2 concentration, Pu(IV) can be desorbed from a silicate mineral in the absence of
389 Fe. However, we also note that 500 μM H_2O_2 is at least an order of magnitude greater than
390 environmental H_2O_2 concentrations. The difference in Pu desorption behavior between quartz at
391 500 μM and 5 μM highlights both the complexity of mineral-contaminant- H_2O_2 reactions and
392 the importance of using environmentally relevant H_2O_2 concentrations when investigating
393 environmental, H_2O_2 -catalyzed reactions.

394 **ENVIRONMENTAL IMPLICATIONS**

395 Previously, it was suggested by Morgenstern and Choppin that the presence of H_2O_2 in the
396 environment may enhance the rate of Pu(V) reduction in natural waters, potentially limiting its
397 environmental mobility.⁶ In the current study, we show that Pu(IV) adsorbed to the surface of
398 goethite experiences a pH-dependent desorption in the presence of environmentally relevant

399 concentrations of H₂O₂. The presence of environmental concentrations of H₂O₂ also caused
400 desorption of Pu from quartz and goethite was but this was far less significant than for goethite.
401 These results suggest that H₂O₂ can catalyze the desorption of mineral associated Pu(IV) in
402 contaminated environments especially in the presence of Fe species. Given the ubiquity of Fe
403 minerals such as goethite in the environment this mechanism may be important in a number of
404 scenarios including: surface water environments experiencing rainfall input as well as seasonal
405 changes in hydrogen peroxide-generating natural organic matter; subsurface environments where
406 bacterial processes generate high levels of H₂O₂; and nuclear waste repositories where H₂O₂ is
407 formed by the effect of radiation on water. Further study is needed to elucidate the Pu desorption
408 mechanism. There is also the potential that this desorption process will be relevant for other
409 redox active radionuclides, such as uranium or neptunium, which show lower environmental
410 mobility in the reduced oxidation state.

411 **ACKNOWLEDGEMENTS**

412 We thank Dr R. Tinnacher (LBNL) for thought provoking discussions and Dr I. Cvijanovic
413 (Carnegie Institution for Science, Stanford) for helpful suggestions. This work was supported by
414 the Subsurface Biogeochemical Research Program of the U.S. Department of Energy's Office of
415 Biological and Environmental Research. Prepared by LLNL under Contract DE-AC52-
416 07NA27344.

417 **SUPPORTING INFORMATION AVAILABLE**

418 Online supporting information, where noted in the text, is available on the internet. This
419 information is available free of charge via the Internet at <http://pubs.acs.org/>.

420

421

422 REFERENCES

423

424 1. Nelson, D. M.; Lovett, M. B., Oxidation state of plutonium in the Irish Sea. *Nature* **1978**,
425 276, (5688), 599-601.

426 2. Montero, P. R.; Sanchez, A. M., Plutonium contamination from accidental release or
427 simply fallout: study of soils at Palomares (Spain). *J Environ Radioactiv* **2001**, 55, (2), 157-165.

428 3. Smith, D. K.; Finnegan, D. L.; Bowen, S. M., An inventory of long-lived radionuclides
429 residual from underground nuclear testing at the Nevada test site, 1951-1992. *J Environ*
430 *Radioactiv* **2003**, 67, (1), 35-51.

431 4. Morris, K.; Butterworth, J. C.; Livens, F. R., Evidence for the remobilization of Sellafield
432 waste radionuclides in an intertidal salt marsh, West Cumbria, UK. *Estuar Coast Shelf S* **2000**,
433 51, (5), 613-625.

434 5. Choppin, G. R., Redox speciation of plutonium in natural waters. *J Radioan Nucl Ch Ar*
435 **1991**, 147, (1), 109-116.

436 6. Morgenstern, A.; Choppin, G. R., Kinetics of the reduction of Pu(V)O_2^+ by hydrogen
437 peroxide. *Radiochim Acta* **1999**, 86, (3-4), 109-113.

438 7. Kersting, A. B.; Efurud, D. W.; Finnegan, D. L.; Rokop, D. J.; Smith, D. K.; Thompson, J.
439 L., Migration of plutonium in ground water at the Nevada Test Site. *Nature* **1999**, 397, (6714),
440 56-59.

441 8. Novikov, A. P.; Kalmykov, S. N.; Utsunomiya, S.; Ewing, R. C.; Horreard, F.; Merkulov,
442 A.; Clark, S. B.; Tkachev, V. V.; Myasoedov, B. F., Colloid transport of plutonium in the far-
443 field of the Mayak Production Association, Russia. *Science* **2006**, 314, (5799), 638-641.

444 9. Santschi, P. H.; Roberts, K. A.; Guo, L. D., Organic nature of colloidal actinides
445 transported in surface water environments. *Environ Sci Technol* **2002**, 36, (17), 3711-3719.

446 10. Neck, V.; Altmaier, M.; Seibert, A.; Yun, J. I.; Marquardt, C. M.; Fanghanel, T.,
447 Solubility and redox reactions of Pu(IV) hydrous oxide: Evidence for the formation of $\text{PuO}_{2+x(s)}$
448 $_{\text{hyd}}$. *Radiochim Acta* **2007**, 95, (4), 193-207.

449 11. Efurud, D. W.; Runde, W.; Banar, J. C.; Janecky, D. R.; Kaszuba, J. P.; Palmer, P. D.;
450 Roensch, F. R.; Tait, C. D., Neptunium and plutonium solubilities in a Yucca Mountain
451 groundwater. *Environ Sci Technol* **1998**, 32, (24), 3893-3900.

452 12. Begg, J. D.; Zavarin, M.; Zhao, P.; Tumey, S. J.; Powell, B.; Kersting, A. B., Pu(V) and
453 Pu(IV) sorption to montmorillonite. *Environ Sci Technol* **2013**, 47, (10), 5146-5153.

454 13. Powell, B. A.; Fjeld, R. A.; Kaplan, D. I.; Coates, J. T.; Serkiz, S. M., Pu(V)O_2^+
455 adsorption and reduction by synthetic magnetite (Fe_3O_4). *Environ Sci Technol* **2004**, 38, (22),
456 6016-6024.

457 14. Lu, N. P.; Reimus, P. W.; Parker, G. R.; Conca, J. L.; Triay, I. R., Sorption kinetics and
458 impact of temperature, ionic strength and colloid concentration on the adsorption of plutonium-
459 239 by inorganic colloids. *Radiochim Acta* **2003**, 91, (12), 713-720.

460 15. Icopini, G. A.; Lack, J. G.; Hersman, L. E.; Neu, M. P.; Boukhalifa, H., Plutonium(V/VI)
461 reduction by the metal-reducing Bacteria *Geobacter metallireducens* GS-15 and *Shewanella*
462 *oneidensis* MR-1. *Appl Environ Microb* **2009**, 75, (11), 3641-3647.

463 16. Zhao, P. H.; Zavarin, M.; Leif, R. N.; Powell, B. A.; Singleton, M. J.; Lindvall, R. E.;
464 Kersting, A. B., Mobilization of actinides by dissolved organic compounds at the Nevada Test
465 Site. *Appl Geochem* **2011**, 26, (3), 308-318.

- 466 17. Keeney-Kennicutt, W. L.; Morse, J. W., The redox chemistry of Pu(V)O₂⁺ interaction
467 with common mineral surfaces in dilute solutions and seawater. *Geochim Cosmochim Acta* **1985**,
468 *49*, (12), 2577-2588.
- 469 18. Sanchez, A. L.; Murray, J. W.; Sibley, T. H., The adsorption of plutonium IV and
470 plutonium V on goethite. *Geochim Cosmochim Acta* **1985**, *49*, (11), 2297-2307.
- 471 19. Silva, R. J.; Nitsche, H., Actinide environmental chemistry. *Radiochim Acta* **1995**, *70-1*,
472 377-396.
- 473 20. Choppin, G. R.; Bond, A. H.; Hromadka, P. M., Redox speciation of plutonium. *J*
474 *Radioanal Nucl Ch* **1997**, *219*, (2), 203-210.
- 475 21. Orlandini, K. A.; Penrose, W. R.; Nelson, D. M., Pu(V) as the stable form of oxidized
476 plutonium in natural waters. *Mar Chem* **1986**, *18*, (1), 49-57.
- 477 22. Powell, B. A.; Duff, M. C.; Kaplan, D. I.; Fjeld, R. A.; Newville, M.; Hunter, D. B.;
478 Bertsch, P. M.; Coates, J. T.; Eng, P.; Rivers, M. L.; Sutton, S. R.; Triay, I. R.; Vaniman, D. T.,
479 Plutonium oxidation and subsequent reduction by Mn(IV) minerals in Yucca Mountain tuff.
480 *Environ Sci Technol* **2006**, *40*, (11), 3508-3514.
- 481 23. Powell, B. A.; Fjeld, R. A.; Kaplan, D. I.; Coates, J. T.; Serkiz, S. M., Pu(V)O₂⁺
482 adsorption and reduction by synthetic hematite and goethite. *Environ Sci Technol* **2005**, *39*, (7),
483 2107-2114.
- 484 24. Lujaniene, G.; Benes, P.; Stamberg, K.; Joksas, K.; Kulakauskaite, I., Pu and Am
485 sorption to the Baltic Sea bottom sediments. *J Radioanal Nucl Ch* **2013**, *295*, (3), 1957-1967.
- 486 25. Buda, R. A.; Banik, N. L.; Kratz, J. V.; Trautmann, N., Studies of the ternary systems
487 humic substances - kaolinite - Pu(III) and Pu(IV). *Radiochim Acta* **2008**, *96*, (9-11), 657-665.
- 488 26. Zavarin, M.; Powell, B. A.; Bourbin, M.; Zhao, P. H.; Kersting, A. B., Np(V) and Pu(V)
489 ion exchange and surface-mediated reduction mechanisms on montmorillonite. *Environ Sci*
490 *Technol* **2012**, *46*, (5), 2692-2698.
- 491 27. Hixon, A. E.; Arai, Y.; Powell, B. A., Examination of the effect of alpha radiolysis on
492 plutonium(V) sorption to quartz using multiple plutonium isotopes. *J Colloid Interf Sci* **2013**,
493 *403*, (0), 105-112.
- 494 28. Kaplan, D. I.; Powell, B. A.; Duff, M. C.; Demirkanli, D. I.; Denham, M.; Fjeld, R. A.;
495 Molz, F. J., Influence of sources on plutonium mobility and oxidation state transformations in
496 vadose zone sediments. *Environ Sci Technol* **2007**, *41*, (21), 7417-7423.
- 497 29. Romanchuk, A. Y.; Kalmykov, S. N.; Aliev, R. A., Plutonium sorption onto hematite
498 colloids at femto- and nanomolar concentrations. *Radiochim Acta* **2011**, *99*, (3), 137-144.
- 499 30. Felmy, A. R.; Moore, D. A.; Rosso, K. M.; Qafoku, O.; Rai, D.; Buck, E. C.; Ilton, E. S.,
500 Heterogeneous reduction of PuO₂ with Fe(II): Importance of the Fe(III) reaction product.
501 *Environ Sci Technol* **2011**, *45*, (9), 3952-3958.
- 502 31. Kirsch, R.; Fellhauer, D.; Altmaier, M.; Neck, V.; Rossberg, A.; Fanghanel, T.; Charlet,
503 L.; Scheinost, A. C., Oxidation state and local structure of plutonium reacted with magnetite,
504 mackinawite, and chukanovite. *Environ Sci Technol* **2011**, *45*, (17), 7267-7274.
- 505 32. Lu, N.; Cotter, C. R.; Kitten, H. D.; Bentley, J.; Triay, I. R., Reversibility of sorption of
506 plutonium-239 onto hematite and goethite colloids. *Radiochim Acta* **1998**, *83*, (4), 167-173.
- 507 33. Hamilton-Taylor, J.; Kelly, M.; Mudge, S.; Bradshaw, K., Rapid remobilization of
508 plutonium from estuarine sediments. *J Environ Radioactiv* **1987**, *5*, (6), 409-423.
- 509 34. Kaplan, D. I.; Powell, B. A.; Gumapas, L.; Coates, J. T.; Field, R. A.; Diprete, D. P.,
510 Influence of pH on plutonium desorption/solubilization from sediment. *Environ. Sci. Tech.* **2006**,
511 *40*, 5937-5942.

- 512 35. McCubbin, D.; Leonard, K. S., Photochemical dissolution of radionuclides from marine
513 sediments. *Mar Chem* **1996**, *55*, 399-408.
- 514 36. Burke, I. T.; Boothman, C.; Lloyd, J. R.; Livens, F. R.; Charnock, J. M.; McBeth, J. M.;
515 Mortimer, R. J. G.; Morris, K., Reoxidation behavior of technetium, iron, and sulfur in estuarine
516 sediments. *Environ Sci Technol* **2006**, *40*, (11), 3529-3535.
- 517 37. Law, G. T. W.; Geissler, A.; Lloyd, J. R.; Livens, F. R.; Boothman, C.; Begg, J. D. C.;
518 Denecke, M. A.; Rothe, J.; Dardenne, K.; Burke, I. T.; Charnock, J. M.; Morris, K.,
519 Geomicrobiological redox cycling of the transuranic element neptunium. *Environ Sci Technol*
520 **2010**, *44*, (23), 8924-8929.
- 521 38. Moon, H. S.; Komlos, J.; Jaffe, P. R., Uranium reoxidation in previously bioreduced
522 sediment by dissolved oxygen and nitrate. *Environ Sci Technol* **2007**, *41*, (13), 4587-4592.
- 523 39. Begg, J. D. C.; Burke, I. T.; Charnock, J. M.; Morris, K., Technetium reduction and
524 reoxidation behaviour in Dounreay soils. *Radiochim Acta* **2008**, *96*, (9-11), 631-636.
- 525 40. Sani, R. K.; Peyton, B. M.; Dohnalkova, A.; Amonette, J. E., Reoxidation of reduced
526 uranium with iron(III) (hydr)oxides under sulfate-reducing conditions. *Environ Sci Technol*
527 **2005**, *39*, (7), 2059-2066.
- 528 41. Balakrishnan, P. V.; Mazumdar, A. S. G., Observations on the action of hydrogen
529 peroxide on trivalent and tetravalent plutonium solutions. *Journal of Inorganic & Nuclear*
530 *Chemistry* **1964**, *26*, (5), 759-765.
- 531 42. Clark, D.; Hecker, S.; Jarvinen, G.; Neu, M., Plutonium. In *The Chemistry of the Actinide*
532 *and Transactinide Elements*, Morss, L.; Edelstein, N.; Fuger, J., Eds. Springer Netherlands:
533 2011; pp 813-1264.
- 534 43. Hagan, P. G.; Miner, F. J., Plutonium peroxide precipitation: Review and current
535 research. In *Actinide Separations*, AMERICAN CHEMICAL SOCIETY: 1980; Vol. 117, pp 51-
536 67.
- 537 44. Shilov, V. P.; Astafurova, L. N.; Garnov, A. Y.; Krot, N. N., Reaction of H₂O₂ with
538 suspensions of Np(OH)₄ and Pu(OH)₄ in alkali solution. *Radiochemistry* **1996**, *38*, (3), 217-219.
- 539 45. Sill, C. W.; Percival, D. R.; Williams, R. L., Catalytic effect of iron on oxidation of
540 plutonium by hydrogen peroxide *Analytical Chemistry* **1970**, *42*, (11), 1273-&.
- 541 46. Cooper, W. J.; Lean, D. R. S., Hydrogen peroxide concentration in a northern lake:
542 photochemical formation and diel variability. *Environ Sci Technol* **1989**, *23*, (11), 1425-1428.
- 543 47. Zika, R. G.; Moffett, J. W.; Petasne, R. G.; Cooper, W. J.; Saltzman, E. S., Spatial and
544 temporal variations of hydrogen-peroxide in Gulf of Mexico waters. *Geochim Cosmochim Ac*
545 **1985**, *49*, (5), 1173-1184.
- 546 48. GonzalezFlecha, B.; Demple, B., Homeostatic regulation of intracellular hydrogen
547 peroxide concentration in aerobically growing *Escherichia coli*. *Journal of Bacteriology* **1997**,
548 *179*, (2), 382-388.
- 549 49. Guillen, F.; Martinez, A. T.; Martinez, M. J., Production of hydrogen-peroxide by aryl-
550 alcohol oxidase from the ligninolytic fungus *Pleurotus eryngii*. *Applied Microbiology and*
551 *Biotechnology* **1990**, *32*, (4), 465-469.
- 552 50. Kok, G. L., Measurements of hydrogen-peroxide in rainwater. *Atmospheric Environment*
553 **1980**, *14*, (6), 653-656.
- 554 51. Watts, R. J.; Finn, D. D.; Cutler, L. M.; Schmidt, J. T.; Teel, A. L., Enhanced stability of
555 hydrogen peroxide in the presence of subsurface solids. *J Contam Hydrol* **2007**, *91*, (3-4), 312-
556 326.

557 52. Li, H. P.; Yeager, C. M.; Brinkmeyer, R.; Zhang, S. J.; Ho, Y. F.; Xu, C.; Jones, W. L.;
558 Schwehr, K. A.; Ootaka, S.; Roberts, K. A.; Kaplan, D. I.; Santschi, P. H., Bacterial production
559 of organic acids enhances H₂O₂-dependent iodide oxidation. *Environ Sci Technol* **2012**, *46*, (9),
560 4837-4844.

561 53. Christensen, H., Calculations simulating spent-fuel leaching experiments. *Nuclear*
562 *Technology* **1998**, *124*, (2), 165-174.

563 54. Amme, M.; Bors, W.; Michel, C.; Stettmaier, K.; Rasmussen, G.; Betti, M., Effects of
564 Fe(II) and hydrogen peroxide interaction upon dissolving UO₂ under geologic repository
565 conditions. *Environ Sci Technol* **2005**, *39*, (1), 221-229.

566 55. Amme, M.; Pehrman, R.; Deutsch, R.; Roth, O.; Jonsson, M., Combined effects of Fe(II)
567 and oxidizing radiolysis products on UO₂ and PuO₂ dissolution in a system containing solid UO₂
568 and PuO₂. *Journal of Nuclear Materials* **2012**, *430*, (1-3), 1-5.

569 56. Voelker, B. M.; Sulzberger, B., Effects of fulvic acid on Fe(II) oxidation by hydrogen
570 peroxide. *Environ Sci Technol* **1996**, *30*, (4), 1106-1114.

571 57. Kwan, W. P.; Voelker, B. M., Decomposition of hydrogen peroxide and organic
572 compounds in the presence of dissolved iron and ferrihydrite. *Environ Sci Technol* **2002**, *36*, (7),
573 1467-1476.

574 58. Hug, S. J.; Leupin, O., Iron-catalyzed oxidation of arsenic(III) by oxygen and by
575 hydrogen peroxide: pH-dependent formation of oxidants in the Fenton reaction. *Environ Sci*
576 *Technol* **2003**, *37*, (12), 2734-2742.

577 59. Voegelin, A.; Hug, S. J., Catalyzed oxidation of arsenic(III) by hydrogen peroxide on the
578 surface of ferrihydrite: An in situ ATR-FTIR study. *Environ Sci Technol* **2003**, *37*, (5), 972-978.

579 60. Pettine, M.; Millero, F. J., Effect of metals on the oxidation of As(III) with H₂O₂. *Mar*
580 *Chem* **2000**, *70*, (1-3), 223-234.

581 61. Powell, B. A.; Dai, Z. R.; Zavarin, M.; Zhao, P. H.; Kersting, A. B., Stabilization of
582 plutonium nano-colloids by epitaxial distortion on mineral surfaces. *Environ Sci Technol* **2011**,
583 *45*, (7), 2698-2703.

584 62. Tinnacher, R. M.; Zavarin, M.; Powell, B. A.; Kersting, A. B., Kinetics of neptunium(V)
585 sorption and desorption on goethite: An experimental and modeling study. *Geochim Cosmochim*
586 *Ac* **2011**, *75*, (21), 6584-6599.

587 63. Lovley, D. R.; Phillips, E. J. P., Availability of ferric iron for microbial reduction in
588 bottom sediments of the freshwater tidal Potomac River. *Appl Environ Microb* **1986**, *52*, (4),
589 751-757.

590 64. Unimin Iota High Purity Quarz Technical Data. [http://www.iotaquartz.com/pdfs/Iota-](http://www.iotaquartz.com/pdfs/Iota-Semi-V1F.pdf)
591 [Semi-V1F.pdf](http://www.iotaquartz.com/pdfs/Iota-Semi-V1F.pdf)

592 65. Kobashi, A.; Choppin, G. R., A study of techniques for separating plutonium in different
593 oxidation states. *Radiochim. Acta* **1988**, *43*, 211-215.

594 66. Noble, R. W.; Gibson, Q. H., Reaction of ferrous horseradish peroxidase with hydrogen
595 peroxide *J. Biol. Chem.* **1970**, *245*, (9), 2409-&.

596 67. Viollier, E.; Inglett, P. W.; Hunter, K.; Roychoudhury, A. N.; Van Cappellen, P., The
597 ferrozine method revisited: Fe(II)/Fe(III) determination in natural waters. *Appl Geochem* **2000**,
598 *15*, (6), 785-790.

599 68. Zhou, M. J.; Diwu, Z. J.; PanchukVoloshina, N.; Haugland, R. P., A stable
600 nonfluorescent derivative of resorufin for the fluorometric determination of trace hydrogen
601 peroxide: Applications in detecting the activity of phagocyte NADPH oxidase and other
602 oxidases. *Analytical Biochemistry* **1997**, *253*, (2), 162-168.

603 69. Invitrogen Amplex® Red Hydrogen Peroxide/Peroxidase Assay Kit.
604 <http://tools.lifetechnologies.com/content/sfs/manuals/mp22188.pdf>
605 70. Pham, A. L. T.; Doyle, F. M.; Sedlak, D. L., Inhibitory effect of dissolved silica on H₂O₂
606 decomposition by iron(III) and manganese(IV) oxides: Implications for H₂O₂-based in situ
607 chemical oxidation. *Environ Sci Technol* **2012**, *46*, (2), 1055-1062.
608 71. Lin, S. S.; Gurol, M. D., Catalytic decomposition of hydrogen peroxide on iron oxide:
609 Kinetics, mechanism, and implications. *Environ Sci Technol* **1998**, *32*, (10), 1417-1423.

610

611

612

613

614

615

616

617

618

619

620

621

622

623

624

625

626

627

628

629

630

631

632

633

634

635

636

637

638

639

640

641

642

643

644

645

646

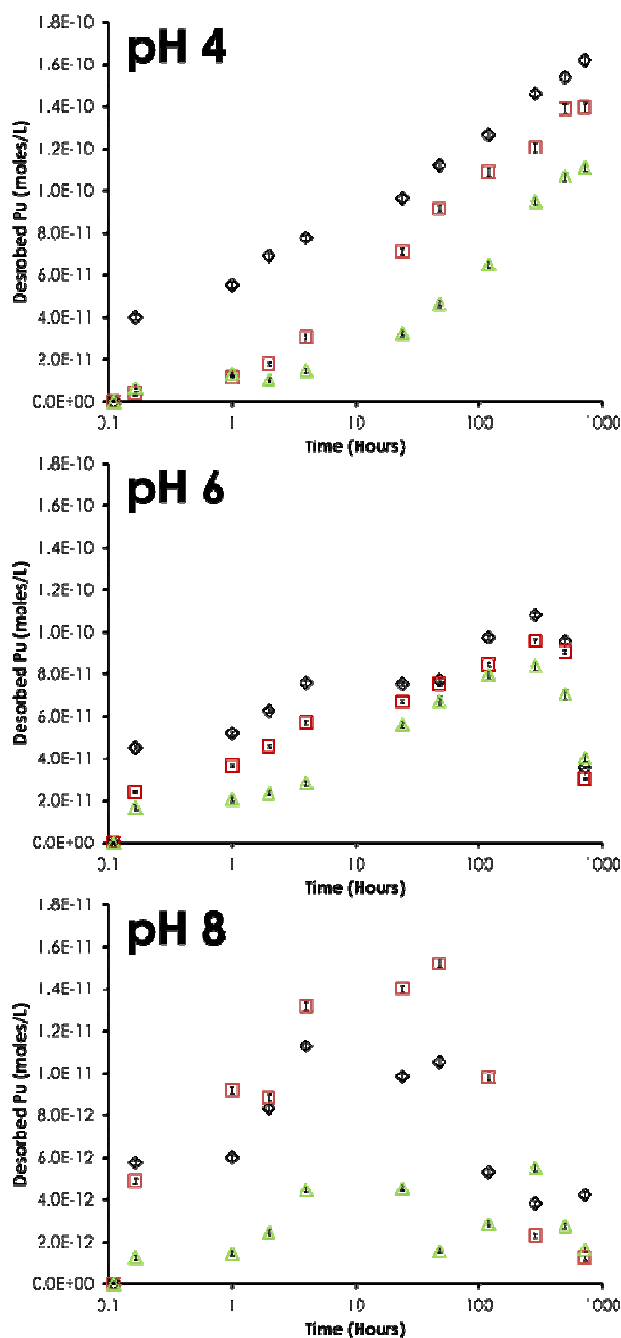
647

648 **Table**
649

Mineral	pH 4	pH 6	pH 8
Goethite	4.42 ± 0.02	5.31 ± 0.02	6.21 ± 0.07
Montmorillonite	6.29 ± 0.28	4.92 ± 0.03	4.48 ± 0.02
Quartz	3.20 ± 0.04	3.50 ± 0.03	3.71 ± 0.03

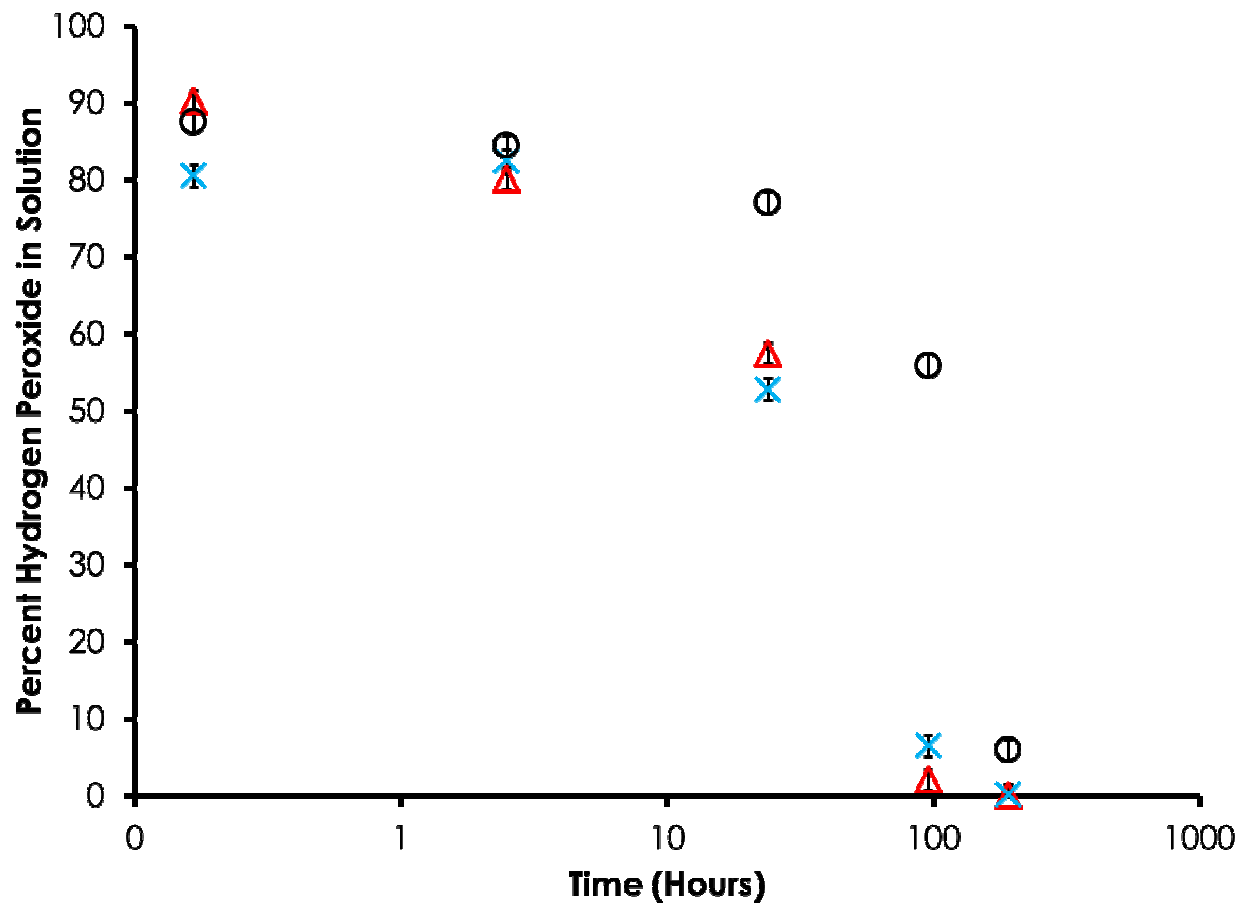
650
651 **Table 1.** Calculated log K_d (mL g⁻¹) Pu(IV) values for goethite, montmorillonite, and quartz as a
652 function of pH value following 21 days' equilibrium in 0.7 mM NaHCO₃, 5 mM NaCl buffer
653 solution. Error bars based on propagation of 2s % LSC uncertainties.

654
655
656
657
658
659
660



662

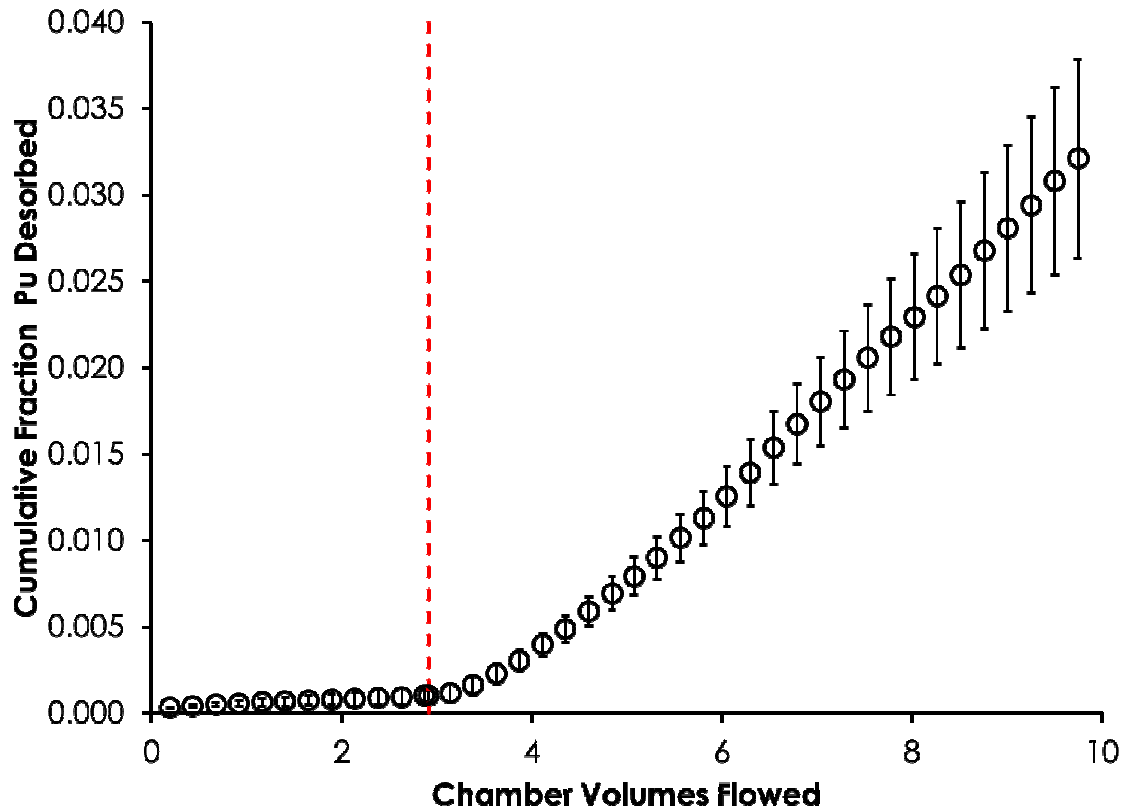
663 **Figure 1.** Desorption of Pu from goethite following addition of: 5×10^{-4} M H_2O_2 (diamonds); 5
 664 $\times 10^{-5}$ M H_2O_2 (squares); and 5×10^{-6} M H_2O_2 (triangles). Experiments performed in 0.7 mM
 665 $NaHCO_3$, 5 mM $NaCl$ buffer solution with 0.1 g L^{-1} goethite. Desorbed Pu calculated as increase
 666 in concentration of solution Pu following addition of H_2O_2 . Error bars based on propagation of 2s
 667 % LSC uncertainties. Please note differences in y-axis scales.



668

669 **Figure 2.** H₂O₂ loss from solution in parallel, Pu-free 0.1 gL⁻¹ goethite / 0.7 mM NaHCO₃, 5 mM
 670 NaCl buffer suspensions. Experiments performed at initial pH values of 4 (triangles); 6 (crosses);
 671 and 8 (circles) and spiked with 5 × 10⁻⁵ M H₂O₂. Errors extrapolated from the standard deviation
 672 of triplicate sample measurement at 192 hours.

673



674

675 **Figure 3.** Experimental results from Pu(IV)–goethite desorption flow-cell experiment performed
 676 with 3×10^{-10} M Pu_{Bulk} and 0.1 g L^{-1} goethite at pH 8. Initially the influent solution was Pu-free
 677 0.7 mM NaHCO_3 , 5 mM NaCl buffer at pH 8. After 3 chamber volumes, the cell was spiked with
 678 1×10^{-5} M H_2O_2 (denoted by dashed red line). Influent flow rate was 0.4 mL min^{-1} (50 minute
 679 average retention time). Error bars based on propagation of LSC uncertainties.

680

681

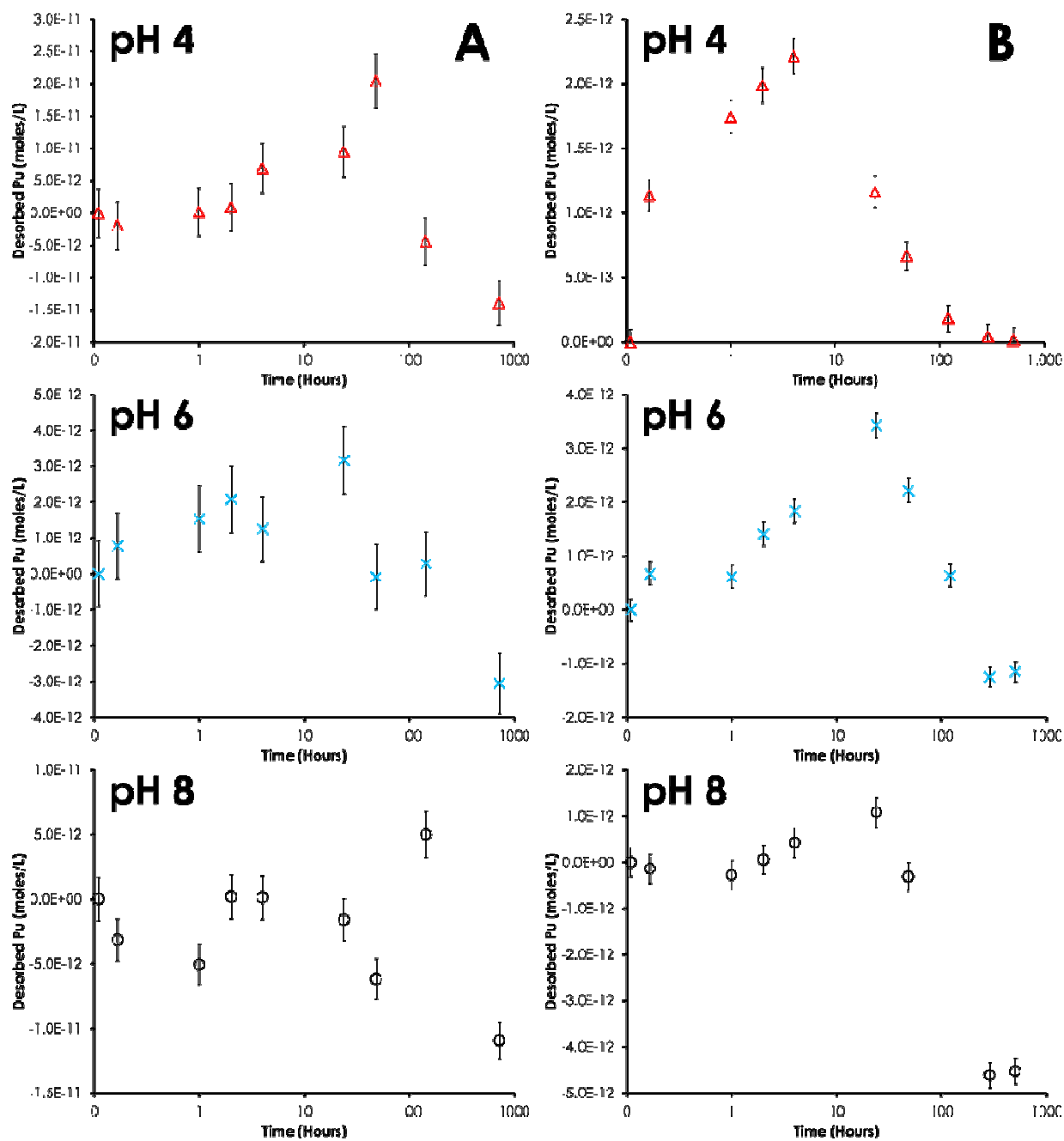
682

683

684

685

686



687

688 **Figure 4.** Desorption of Pu from (A) quartz and (B) montmorillonite following addition of $5 \times$
 689 10^{-6} M H_2O_2 . Experiments performed in 0.7 mM NaHCO_3 , 5 mM NaCl buffer solution with 1 g
 690 L^{-1} mineral. Note the difference in y-axis scale between the two minerals and the different pH
 691 values. Values may be negative if Pu concentrations fall below the concentration at the start of
 692 the experiment. Error bars based on propagation of 2s % LSC uncertainties.

